

## Similarity in the Equilibrium Boundary Layer in Accelerating Free Stream Velocity

H.Tokunaga<sup>1</sup>, T. Kameda<sup>2</sup> and S. Mochizuki<sup>3</sup>

<sup>1</sup>Graduate School of Science and Engineering  
 Yamaguchi University, 2-16-1 Tokiwadai Ube 755-8611, Japan

<sup>2</sup>Department of Mechanical Engineering  
 Kinki University, 1 Umenobe Takaya 739-2116, Japan

<sup>3</sup>Graduate School of Science and Engineering  
 Yamaguchi University, 2-16-1 Tokiwadai Ube 755-8611, Japan

### Abstract

Similarity of the near wall turbulence has been investigated in an equilibrium boundary layer under a favourable pressure gradient. The wall shear stress was measured by drag balance, sublayer plate and Preston tube methods, etc. The similarity was discussed using the velocity scale based on the momentum equation. For the pressure gradient parameter of  $P^+ = -3.51 \times 10^{-3}$ , it was confirmed a modified logarithmic law is applicable in the near wall and the Kármán constant is  $\kappa = 0.46$ . For the streamwise turbulent intensity profiles, it is seen that the normalized profile with the velocity scale shows reasonable similarity in the limited range of  $-0.008 < P^+ \leq 0.006$ .

### Introduction

In a flow subjected to a favourable pressure gradient in which static pressure to a flow is decreased to the streamwise direction, pressure gradient accelerates the flow in streamwise direction. Such kind of flow is frequently observed near the leading edge of wings and nose of aircrafts, bow of submarines and suction nozzle of fluid machines such as pumps and turbines. Attempt to investigate the development of a boundary layer and establish the similarity laws of the mean velocity and turbulence has been made for prediction and control of turbulent boundary layers.

Experimental investigation for the boundary layer under the favourable pressure gradient (hereinafter, referred as F.P.G. flow) was conducted by Metzger et al. [1] and Dixit et al. [2]. They already discussed on the effect of the favourable pressure gradient to the law of the wall and concluded that the law of the wall is well-established even though the favourable pressure gradient acts to the flow. However, some serious problem has been remaining in their experimental approach. It can be pointed out that they used Clauser diagram method to estimate the local skin friction coefficient.

In the present study, F.P.G. flow has been satisfied the conditions of the equilibrium boundary layer proposed by J.C. Rotta [3]. The wall shear stress is measured by several methods like drag balance, sublayer plate and Preston tube methods etc. In order to reveal the near wall turbulent structure, the similarity laws will be discussed by use of two velocity scales based on wall shear stress and momentum balance. In addition, the turbulent kinetic energy budget will be investigated to explain the effect of the favourable pressure gradient.

### Experimental Equipment and Conditions

Figure 1 shows the flow field, nomenclature and coordinate system. The experiment was conducted at Eiffel type wind tunnel. The test section has 910 mm in width and 6000 mm in length.  $y$  is the distance in the height direction from the origin placed on the test plate,  $x_0$  is the distance in the streamwise direction from the leading edge of the test plate.  $U_e$  is the free stream velocity at each streamwise position. At  $x_0 = 2300$ mm, the free stream velocity was symbolized by  $U_0 (=8$ m/s). The tripping wire was placed at  $x_0 = 150$ mm to establish a turbulent boundary layer in an early stage. The turbulent boundary layer under a zero pressure gradient (hereinafter, referred as Z.P.G. flow) is developing in the upstream region ( $x_0 < 2300$ mm). The favourable pressure gradient is held in the range of  $2300$ mm  $\leq x_0 < 5000$ mm. The Reynolds number  $R_\theta (= U_e \theta / \nu, \nu$  is kinematic viscosity.) based on the momentum thickness  $\theta$  is 2200 at  $x_0 = 2300$ mm. In the exit region of  $x_0 \geq 5000$ mm, the static pressure in the diffuser portion is gradually recovered to atmospheric pressure.

Figure 2 gives the variation of the free stream velocity  $U_e$  to the streamwise distance  $x_0$ . The free stream velocity  $U_e$  is normalized with  $U_0$ . In the zero pressure gradient region,  $U_e / U_0$  has almost constant value of 1. On the other hand,  $U_e / U_0$  gradually increases with the streamwise distance in the favorable pressure gradient region. It is clear that the variation of  $U_e / U_0$

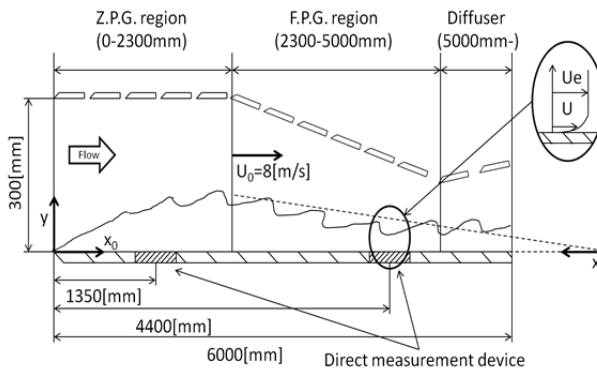


Figure 1. Flow field, nomenclature and coordinate system

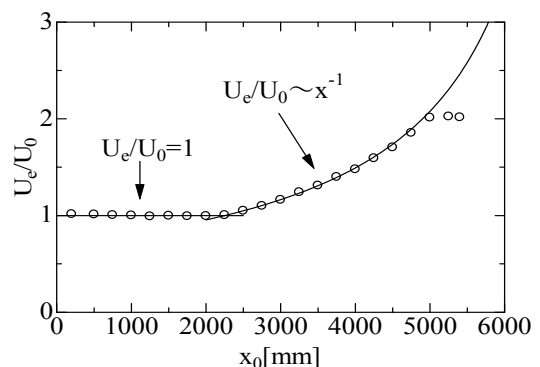


Figure 2. Variation of free stream velocity to streamwise distance

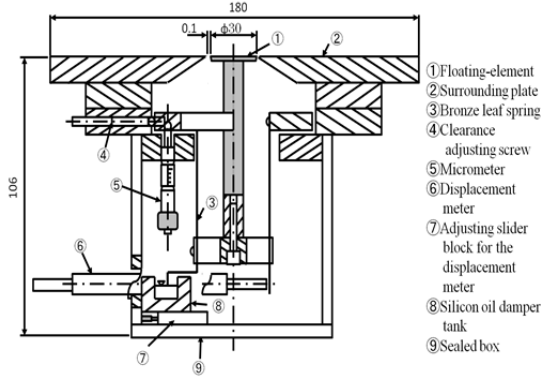


Figure 3. Floating element device for drag balance.

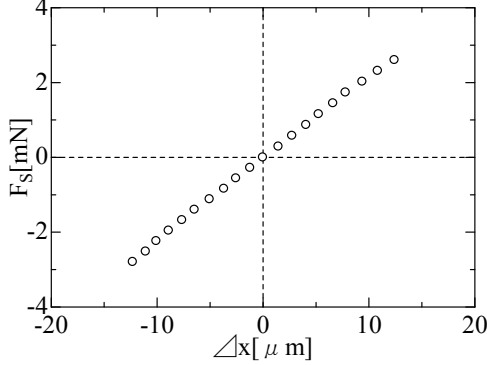


Figure 4. Static calibration curve for drag balance measurement.

can be represented as an inverse of the streamwise distance  $x$  from a virtual sink point.

The measurement of velocity components was carried out using a single hot wire probe operated with a constant temperature anemometer. The hot wire sensor was a tungsten filament of  $2.5\mu\text{m}$  in diameter and  $0.5\text{mm}$  in active length. The signal from the anemometer was stored in a PC after it was converted from analogue signals to digital signals by an AD converter. The stored time is 40sec and the sampling frequency is 10 kHz.

The wall shear stress was measured with the drag balance by a floating element device as shown in Fig.3, sub-layer plate and a Preston tube. The floating element device has a parallel link mechanism, so that the element is supported by two spring leaves. The diameter of the element is  $30\text{mm}$ , the gap size between the surrounding plate and element is  $0.1\text{mm}$ , and the lip size is  $1\text{mm}$ . The static calibration test was performed to measure the displacement  $\Delta x$  of the element arose by any known tangential force which acts on the element surface. The displacement was measured by a capacitance displacement meter. The static calibration curve is shown in Fig.4. The relation between the tangential force and the displacement is linear. By using the relation, the wall shear stress is directly measured from the displacement. In preliminary experiment, it was made clear that the local skin friction coefficient measured with the drag balance is strongly affected to the lip force acting on the lateral area of the element. Therefore, the local skin friction coefficient was calculated by subtracting the lip force integrated the pressure distribution on the lateral area from the force acting on the element estimated from the static calibration curve. The sublayer plate consists of a thin rectangular plate. The plate size is  $15\text{mm}$  in width,  $5\text{mm}$  in length and  $0.1$  and  $0.2\text{mm}$  in thickness. The wall shear stress  $\tau_w$  was determined from the pressure difference  $\Delta P$  between front and back face of the plate. The calibration Eq.(1) was referred from the paper titled as ‘‘Sublayer Plate Method for Local Wall Shear Stress Measurement’’ presented in 19<sup>th</sup> AFMC.

$$Y^* = f(X^*),$$

$$\text{where } Y^* = \log\left(\frac{\tau_w h^2}{\rho v^2}\right) \text{ and } X^* = \log\left(\frac{\Delta P h^2}{\rho v^2}\right) \quad (1)$$

In Eq.(1),  $\rho$  is fluid density and  $h$  is the height of the plate. The Preston tube is made of a stainless pipe with  $1.5\text{mm}$  in outer diameter and  $1\text{mm}$  in inner diameter. The static pressure is measured from a pressure tap drilled in the wall. These devices are set-up at  $x_0=1350\text{mm}$  in the zero pressure gradient region and  $4400\text{mm}$  in the favourable pressure gradient region.

### Velocity Scales near a Wall

The traditional velocity scale called as the friction velocity  $u_\tau$  is defined as follow.

$$u_\tau = \sqrt{\tau_w / \rho} \quad (2)$$

In high Reynolds number, it is generally known that for Z.P.G. flow the Reynolds shear stress  $-\overline{uv}$  is almost equal to the wall shear stress near the wall and the streamwise mean velocity gradient  $\partial U / \partial y$  is scaled with the friction velocity  $u_\tau$  and height distance  $y$ . So, it has been believed that the streamwise mean velocity profile becomes a well-known logarithmic function called as the log law,

$$U^+ = \frac{1}{\kappa_0} \ln y^+ + C_0, \text{ where } U^+ = \frac{U}{u_\tau} \text{ and } y^+ = \frac{y u_\tau}{\nu}. \quad (3)$$

The standard Kármán constant  $\kappa_0$  and additive constant  $C_0$  is  $\kappa_0 = 0.384$  and  $C_0 = 4.17$  [4].

In the turbulent boundary layer under the pressure gradient, the Reynolds shear stress profile depends on the pressure gradient. Therefore, it is thought that the streamwise mean velocity gradient isn't scaled in the same manner as the zero pressure gradient. Nakamura et al.[5] introduced a new velocity scale from the momentum balance using the Reynolds averaged Navier-Stokes equations for the turbulent boundary layer under the adverse pressure gradient(hereinafter, referred as A.P.G. flow) and proposed a modified logarithmic function. We will discuss whether the new velocity scale is applicable for F.P.G. flow. The new velocity scale and the modified logarithmic function are explained briefly as follow. The Reynolds averaged equation applied the boundary layer approximation deduces to Eq. (4).

$$U \frac{\partial U}{\partial x} + V \frac{\partial U}{\partial y} = -\frac{1}{\rho} \frac{dP_e}{dx} + \frac{1}{\rho} \frac{\partial \tau}{\partial y}, \text{ where } \tau = -\overline{\rho uv} + \mu \frac{\partial U}{\partial y} \quad (4)$$

As a first approximation, it is assumed that the streamwise mean velocity  $U$  can be replaced by Eq. (3). The normal mean velocity  $V$  might be given as Eq. (5) near the wall region from order analysis.

$$V = -\frac{dU_e}{dx} y \quad (5)$$

By substituting Eqs.(3) and (5) to Eq.(4) and integrating from 0 to any height near the wall with respect to  $y$ , the shear stress  $\tau$  can be written by

$$\tau = \tau_w \left( 1 + \left[ 1 - \left( \frac{1}{\kappa_0} \ln y^+ + C_0 - \frac{2}{\kappa_0} \right) \omega \right] P^+ y^+ \right). \quad (6)$$

Here, the shear stress is approximated as  $\tau = -\overline{\rho uv}$  except for the viscous sublayer,  $\omega$  is the friction parameter ( $= u_\tau / U_e$ ) and  $P^+$  is pressure gradient parameter ( $= \nu / (\rho u_\tau^2) dP_e / dx$ ). The new velocity scale is defined as

$$u_s = u_\tau \sqrt{1 + \left[ 1 - \left( \frac{1}{\kappa_0} \ln y^+ + C_0 - \frac{2}{\kappa_0} \right) \omega \right] P^+ y^+}. \quad (7)$$

Furthermore, by applying the Maclaurin's expansion with respect to  $P^+$  for Eq. (7), the new velocity scale is rewritten by

$$u_s = u_\tau \left( 1 + \frac{1}{2} \left[ 1 - \left( \frac{1}{\kappa_0} \ln y^+ + C_0 - \frac{2}{\kappa_0} \right) \omega \right] P^+ y^+ \right). \quad (8)$$

From Eq.(8), it is confirmed that  $u_s$  is equal to  $u_t$  as  $P^+$  tends to zero. By integrating the non-dimensional streamwise mean velocity gradient scaled with the new velocity scale and mean height distance, the modified logarithmic function is proposed as

$$U^+ = \frac{1}{\kappa} \ln y^+ + \frac{1}{2\kappa} \left\{ (1 - C_0 \omega) + 3 \frac{\omega}{\kappa_0} \right\} P^+ y^+ - \frac{1}{2\kappa} \frac{\omega}{\kappa_0} P^+ y^+ \ln y^+ + C_p \quad (9)$$

Here, the Kármán constant  $\kappa$  and additive constant  $C_p$  are determined experimentally. In A.P.G. flow with  $P^+ = 2.74 \times 10^{-3}$ , Nakamura et al.[5] reported  $\kappa = 0.45$  and  $C_p = 5.3$ .

## Results and Discussions

### Local Skin friction coefficient

Figure 5 shows the local skin friction coefficient  $c_f$  at  $x_0 = 1350$  mm ( $R_0 = 1397$ ) and 4400 mm ( $R_0 = 2179$ ). In Fig.5, the data calculated from Ludwig-Tillmann formula (10) and the integral momentum equation (11) are included.

$$c_f = 0.246 \times 10^{-0.673H} R_0^{-0.268} \quad (10)$$

$$c_f = 2 \frac{d\theta}{dx} + 2 \frac{\theta}{U_e} \frac{dU_e}{dx} (H + 2) \quad (11)$$

Also, the solid line indicates the semi-empirical formula proposed by Osaka et al.[6] for Z.P.G. flow.

$$\frac{1}{c_f} = 20.03(\log R_0)^2 + 17.24(\log R_0) + 3.71 \quad (12)$$

At  $x_0 = 1350$  mm in the region of the zero pressure gradient, the value of the drag balance is well consistent with those by other several methods and Eq.(12) within a few percent. At  $x_0 = 4400$  mm in the region of the favourable pressure gradient, the data of the drag balance, Preston tube and Eq.(10) are within a few percent, but the data of Eq.(11) and the sublayer plate method takes larger and lower values, respectively. All the data comprehensively takes large value compared with that of Eq.(12). It is explained that the large velocity gradient at the wall is arose by the acceleration due to the favourable pressure gradient and the local skin friction coefficient is increased due to the pressure gradient at  $R_0 = 2179$ . In the present study, the local skin friction coefficient on the drag balance was adopted in the following discussions. Then, the pressure gradient parameter was evaluated as  $P^+ = -3.51 \times 10^{-3}$ .

### Reynolds Shear Stress Profile

The Reynolds shear stress profiles are normalized with the inner scales (the friction velocity and viscous length) and shown in Fig. 6 in order to compare with Eq. (6). In Fig.6, the data of Z.P.G. flow is included, and Eq. (6) is drawn as the solid line. The data for F.P.G. flow apparently takes lower value compared with that of Z.P.G. flow. The solid line shows the same tendency with the data of F.P.G. flow, but the value is overestimated rather than it. The difference might be due to viscous effect because the present

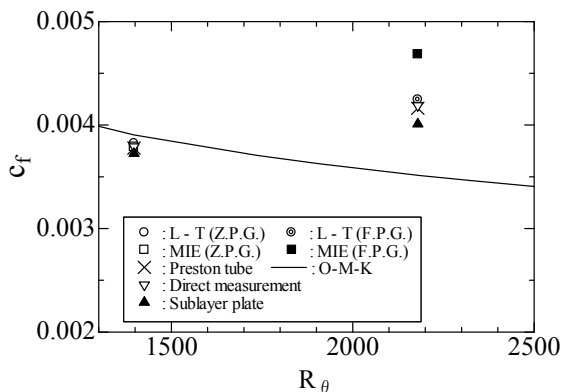


Figure 5. Local skin friction coefficient as a function of  $R_0$ .

experiment has performed in low Reynolds number.

### Logarithmic Mean Velocity Profile

Figure 7 shows the logarithmic mean velocity profile in F.P.G. flow to verify Eq. (9). Also, in Fig.9 Eq. (3) is included to compare with Eq. (9). The Kármán constant in Eq. (9) is calculated from the inverse of the non-dimensional streamwise mean velocity gradient and is  $\kappa = 0.46$ . The additive constant is determined by fitting the Eq.(9) substituted  $\kappa = 0.46$  to the data and is given as  $C_p = 5.1$ . The extent ( $70 \leq y^+ \leq 140$ ) of the modified log law region is wider than that of the classical log law region and it is confirmed experimentally that the modified log function can be applied in the F.P.G. flow. It should be noted that the Kármán constant is close to the value of A.P.G. flow although it has been expected to take a lower value because of the compression of eddies due to a strain rate  $\partial V / \partial y < 0$ .

### Streamwise Turbulent Intensity Profile

Figure 8 shows the streamwise turbulent intensity profiles. The intensity  $u_{ms}$  and height  $y$  are normalized with two velocity scales ( $u_t$  and  $u_s$ ) and viscous length, respectively. Also, the data for Z.P.G. flow is included in Fig.9. The profile normalized with  $u_t$  is shifted below from that of Z.P.G. flow as  $y^+$  increases. On the other hand, it is seemed that the one normalized with  $u_s$  is similar with that of Z.P.G. flow except for the outer layer.

Next, the non-dimensional streamwise turbulent intensity at the height of  $y^+ = 100$  is investigated for the dependency of the pressure gradient parameter. The height is within the range where the log law exists in the range of  $y^+ \gg 1$ . Figures 9 and 10 give the variation of the streamwise turbulent intensity normalized with the two velocity scales at  $y^+ = 100$  to the pressure gradient parameter. In addition, the data of Nakamura et al.[5] and Monty et al.[7] for A.P.G. flows and Misu et al.[8] for F.P.G. flows are plotted in these figures. In Fig.9, the value of  $u_{ms} / u_t$  increases linearly with the pressure gradient parameter. The

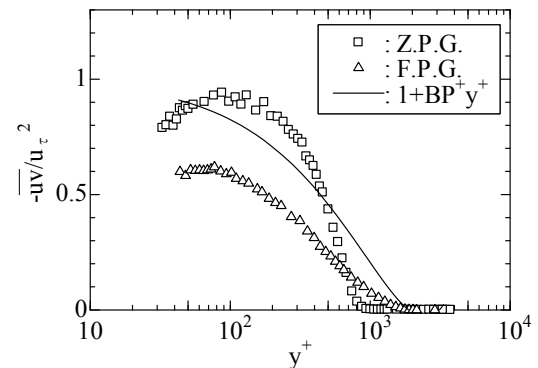


Figure 6. Reynolds shear stress profile

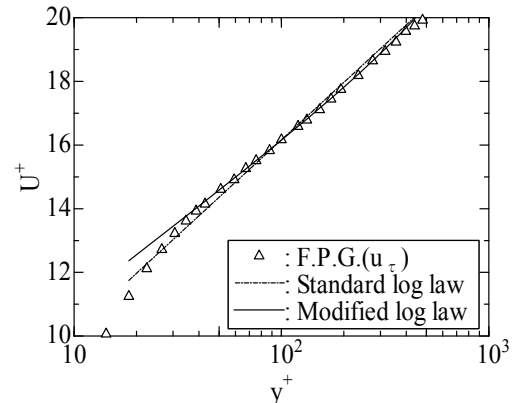


Figure 7. Logarithmic mean velocity profile

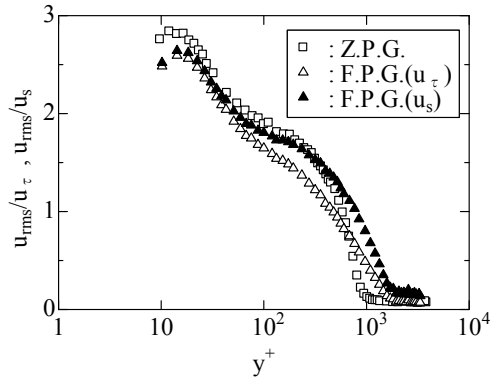


Figure 8. Streamwise turbulent intensity profile

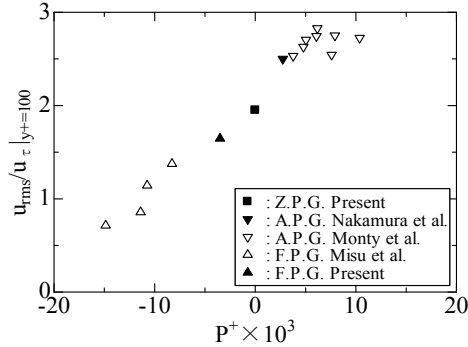


Figure 9. Variation of streamwise turbulent intensity normalized with friction velocity at  $y^+=100$  to pressure gradient parameter

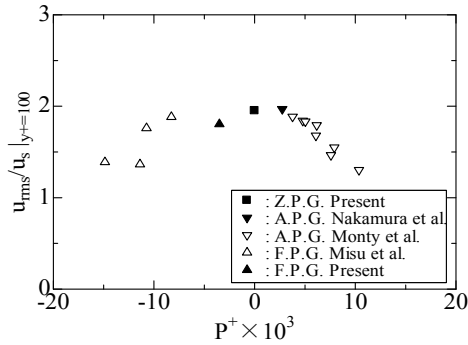


Figure 10. Variation of streamwise turbulent intensity normalized with new velocity scale at  $y^+=100$  to pressure gradient parameter

decrease of the value in the range ( $P^+ < 0$ ) of F.P.G. flow means that the relaminarization of the turbulent flow is progressed as the absolute value of the pressure gradient parameter increases. Contrastively, the value of  $u_{rms}/u_s$  in Fig.10 becomes almost constant in the range of  $-0.008 < P^+ \leq 0.006$ . In this range, it is expected that the profiles become similar regardless of the pressure gradient parameter.

### Turbulent Kinetic Energy Balance

The discrepancy of the streamwise turbulent intensity profile normalized with the friction velocity between F.P.G. flow and Z.P.G. flow is investigated from the turbulent kinetic energy equation. Near the wall, the turbulent kinetic energy equation is approximately balanced by the turbulent energy production and dissipation rate. They are normalized with the friction velocity and boundary layer thickness, and represented as follow.

$$\text{Turbulent energy production: } \text{Pro} = -uv \frac{\partial U}{\partial y} \times \frac{\delta}{u_i^3}$$

$$\text{Turbulent energy dissipation rate: } \text{Dis} = \varepsilon \times \frac{\delta}{u_i^3}$$

The dissipation rate is calculated approximately by the assumption of the existence of inertial subrange and use of the Kolmogorov constant of 0.5. Figure 11 gives the profiles of them

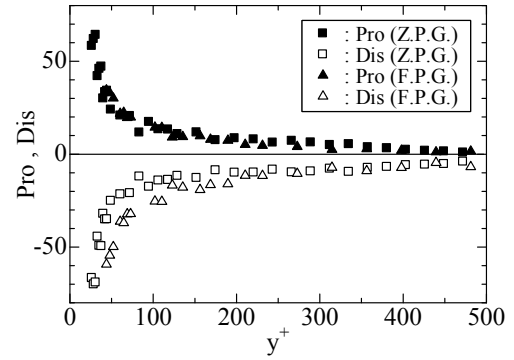


Figure 11. Turbulent kinetic energy balance

near the wall for F.P.G. and Z.P.G. flows. For Z.P.G. flow, the production and dissipation is almost balanced each other except for the viscous sublayer, but for F.P.G. flow the dissipation is twice as large as the production. It is thought that the decrease of the non-dimensional streamwise turbulent intensity is arose by the imbalance due to the higher contribution of the dissipation.

### Conclusions

In this paper, we investigated the applicability of the velocity scale based on the momentum balance to the mean velocity and turbulent intensity profiles near the wall for F.P.G. flow. For the pressure gradient parameter of  $P^+ = -3.51 \times 10^{-3}$ , it was confirmed the modified logarithmic law is applicable for the near wall flow. The Kármán constant is  $\kappa = 0.46$  and close to that for A.P.G. flow of  $P^+ = 2.74 \times 10^{-3}$ . For the streamwise turbulent intensity profiles, it was expected that the normalized profile with the velocity scale shows reasonable similarity in the limited range of  $-0.008 < P^+ \leq 0.006$ .

### References

- [1] Mezger, M, Lyons, A. and Fife, P., Mean Momentum Balance in Moderately Favourable Pressure Gradient Turbulent Boundary Layers, *J. Fluid Mech.*, **617**, 2008, 107-140.
- [2] Dixit, S. and Ramesh, O. N., Pressure-Gradient-Dependent Logarithmic Laws in Sink Flow Turbulent Boundary Layers, *J. Fluid Mech.*, **615**, 2008, 445-475.
- [3] Rotta, J.C., *Turbulent Boundary Layers in Incompressible Flow*, Progress in Aeronautical Science, Vol.2, 1962, Pergamon.
- [4] Nagib H.M. and Chauhan, K.A., Variation of Von Kármán Coefficient in Canonical Flows, *Physics of Fluids*, **20**, 2008, No.101518.
- [5] Nakamura, T., Kameda, T. and Mochizuki, S., Effect of an Adverse Pressure Gradient on the Local Similarity for a Turbulent Boundary Layer, *Transactions of Japan Society of Mechanical Engineers*, **77-775**, 2011, 771-780.
- [6] Osaka, H, Kameda, T. and Mochizuki, S., Re-examination of the Reynolds-Number-Effect on the Mean Flow quantities in a Smooth Wall Turbulent Boundary Layer, *JSME International Journal, Series B*, **41-1**, 1998, 123-129.
- [7] Monty J.P., Harun Z. and Marusic I., "A Parametric Study of Adverse Pressure Gradient Turbulent Boundary Layers", *International Journal of Heat and Fluid Flow*, **32**, 2011, 575-595.
- [8] Misu I., Sada N., Yatabe T., Correlation between Velocities and Wall Shear Stress in the Bursting under Favourable Pressure Gradients, *Transactions of Japan Society of Mechanical Engineers*, **65-632**, 1999, 1312-1317.

